

Three-body scattering Unitarity-based approach

Mikhail Mikhasenko

CERN, Switzerland

May 9th, 2019

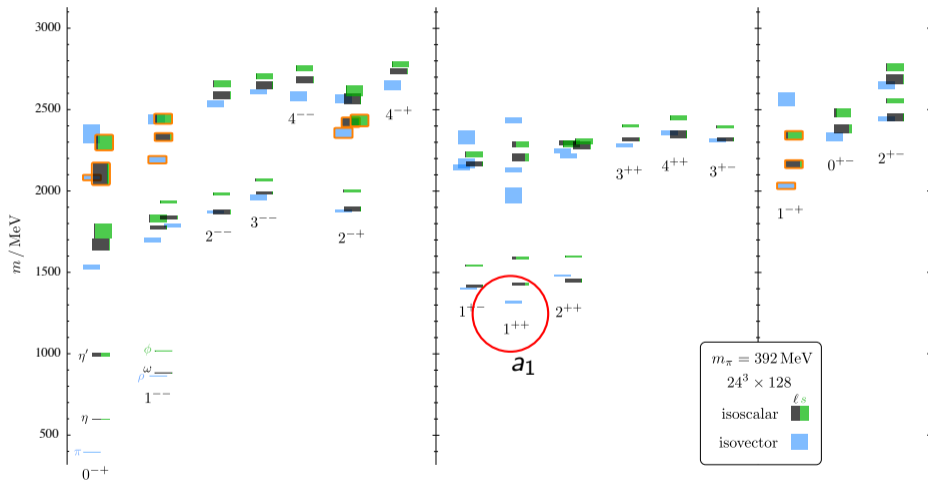


Content

- 1 Unitarity constraint
- 2 Final-state interaction
- 3 Three-particle scattering
- 4 Analysis of the 1^{++} sector

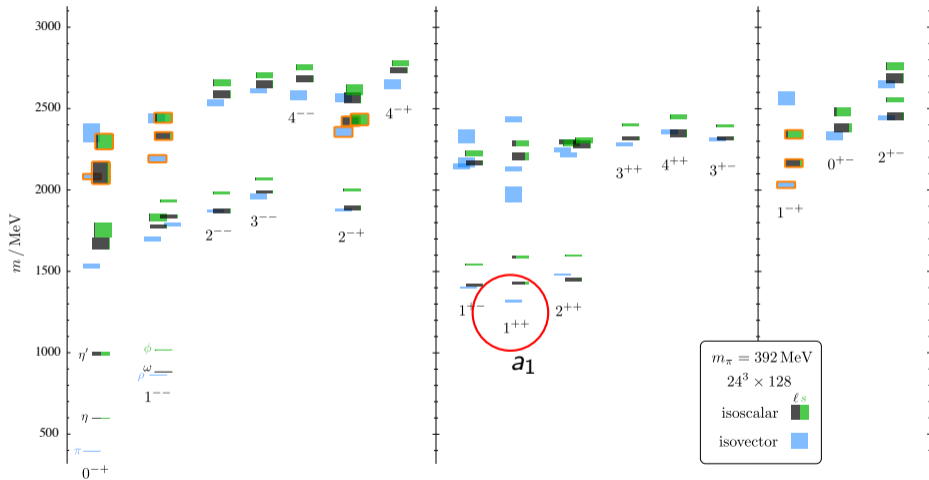
Hadronic excitations from Lattice QCD

[Dudek et al., PRD 88, 094505 (2013)]

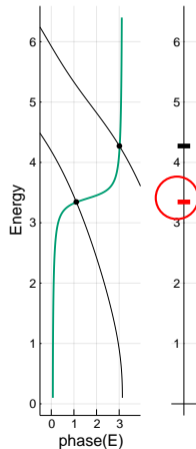


Hadronic excitations from Lattice QCD

[Dudek et al., PRD 88, 094505 (2013)]

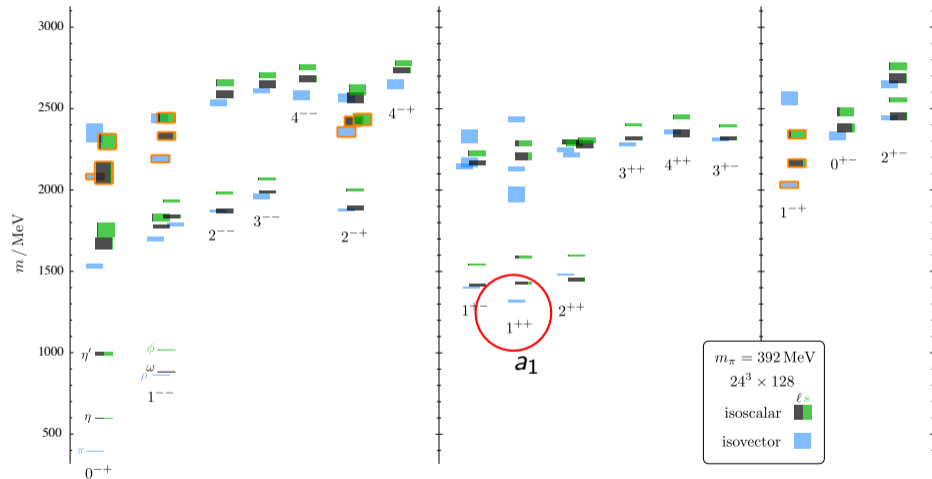


- no width
- mass is not well defined

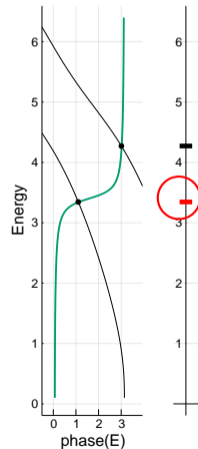


Hadronic excitations from Lattice QCD

[Dudek et al., PRD 88, 094505 (2013)]



- no width
- mass is not well defined



Meanwhile, the first $\rho\pi$ scattering – $l = 2$ [A.Woss, et al. JHEP 1807 (2018) 043]

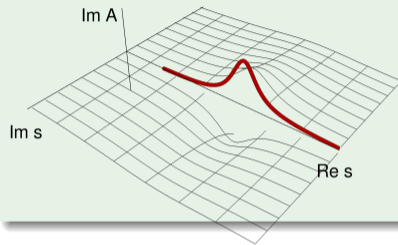
Unitarity of the scattering amplitude

unitarity cut, poles of resonances, dispersive relations

[books by Martin-Spearman, Collins, Gribov]

Resonances = Poles at the Complex plane

Example: Breit-Wigner amplitude

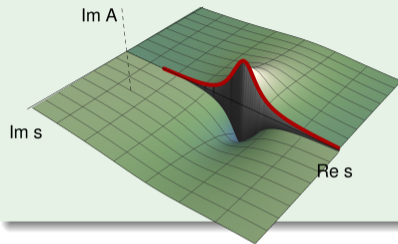


Features of the complex s plane:

- $s = E^2$ – the total inv.mass squared
- The Real axis \rightarrow physical world
- The Imaginary axis \rightarrow analytical continuation

Resonances = Poles at the Complex plane

Example: Breit-Wigner amplitude

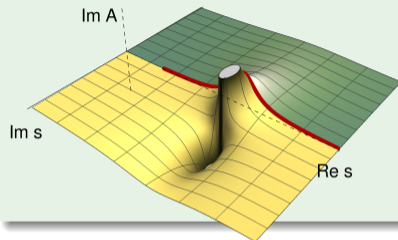


Features of the complex s plane:

- $s = E^2$ – the total inv.mass squared
- The Real axis \rightarrow physical world
- The Imaginary axis \rightarrow analytical continuation

Resonances = Poles at the Complex plane

Example: Breit-Wigner amplitude



Features of the complex s plane:

- $s = E^2$ – the total inv.mass squared
- The Real axis \rightarrow physical world
- The Imaginary axis \rightarrow analytical continuation

Unitarity constraints for the **two-body** scattering

- $\hat{S}^\dagger \hat{S} = \hat{\mathbb{I}} \quad \hat{S} = \hat{\mathbb{I}} + i\hat{T}$
- $T(s, t) = \langle p'_1 p'_2 | \hat{T} | p_1 p_2 \rangle$
- Partial-wave expansion ...
- The final form

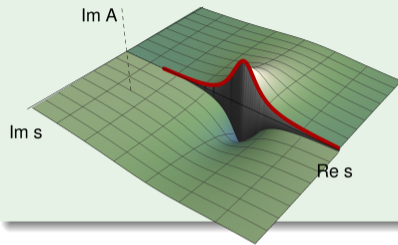
$$\hat{T} - \hat{T}^\dagger = i\hat{T}^\dagger \hat{T}$$

$$T(s, t) - T^\dagger(s, t) = \int d\Phi_2 T^\dagger(s, t') T(s, t'')$$

$$t_l - t_l^\dagger = t_l^\dagger \rho(s) t_l$$

Resonances = Poles at the Complex plane

Example: Breit-Wigner amplitude



Features of the complex s plane:

- $s = E^2$ – the total inv.mass squared
- The Real axis \rightarrow physical world
- The Imaginary axis \rightarrow analytical continuation

Unitarity constraints for the **two-body** scattering

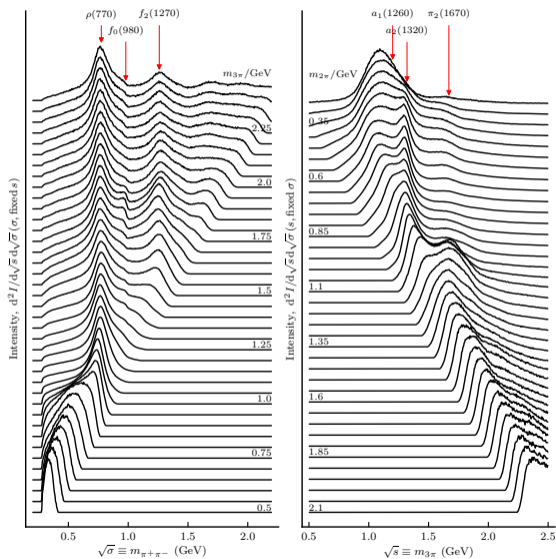
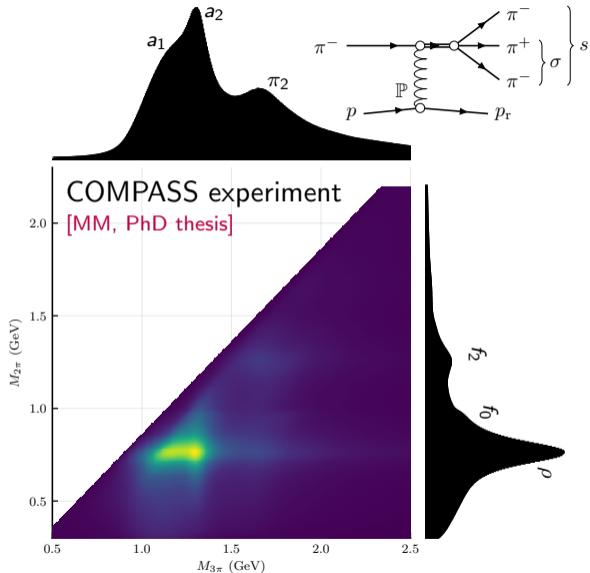
- $\hat{S}^\dagger \hat{S} = \hat{\mathbb{I}} \quad \hat{S} = \hat{\mathbb{I}} + i\hat{T}$
- $T(s, t) = \langle p'_1 p'_2 | \hat{T} | p_1 p_2 \rangle$
- Partial-wave expansion ...
- The final form

$$\hat{T} - \hat{T}^\dagger = i\hat{T}^\dagger \hat{T}$$

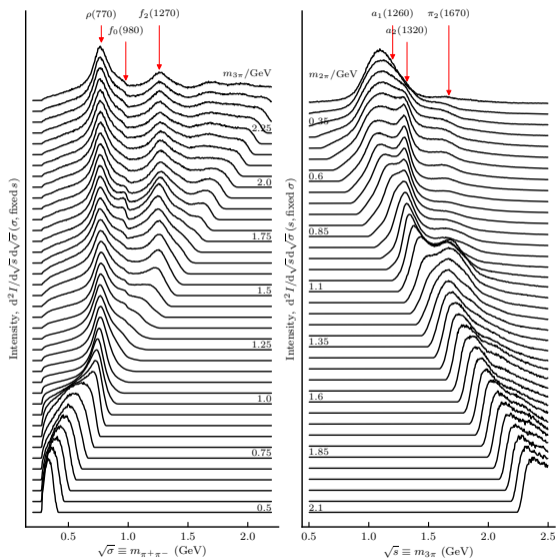
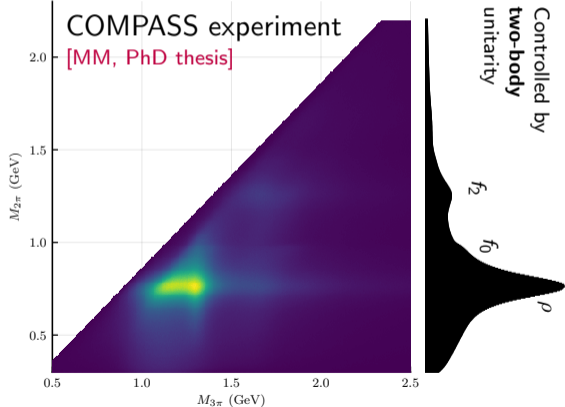
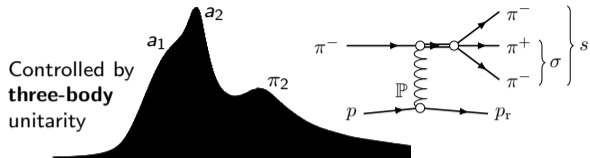
$$T(s, t) - T^\dagger(s, t) = \int d\Phi_2 T^\dagger(s, t') T(s, t'')$$

$$t_l - t_l^\dagger = t_l^\dagger \rho(s) t_l$$

Three-particle interaction: resonances are everywhere



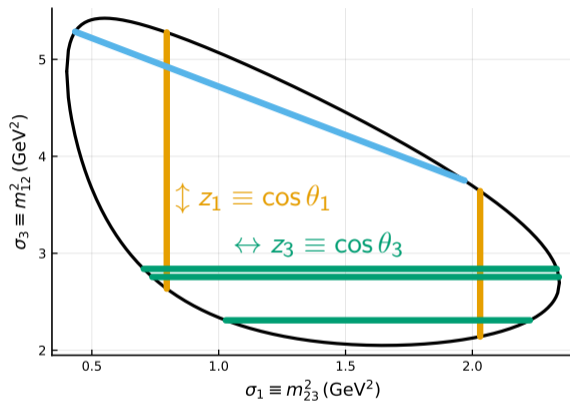
Three-particle interaction: resonances are everywhere



Three-body decay Final-state interaction

isobar model, rescattering, ladder of exchanges

Three-body decay



Decay amplitude – $\langle p_1 p_2 p_3 | \hat{T} | p_0 \rangle$

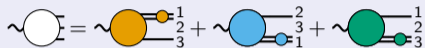
$$\begin{array}{c}
 \sim \text{circle with three external lines} = D_{M\lambda}^{J*}(\alpha, \beta, \gamma) F_\lambda(s, \sigma_1, \sigma_2) \\
 \xrightarrow{\text{scalars}} F(\sigma_1, \sigma_2)
 \end{array}$$

Dalitz plot variables

- Subchannel resonances are bands.
- Angular distribution along the bands determined by angular momenta.

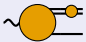
Partial-waves vs Isobar representation

Isobar representation



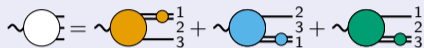
$$F(\sigma_1, \sigma_2) = F^{(1)}(\sigma_1, \sigma_2) + F^{(2)}(\sigma_1, \sigma_2) + F^{(3)}(\sigma_1, \sigma_2)$$

$$= \sum_l^{\text{few}} \sqrt{2l+1} P_l(z_1) a_l^{(1)}(\sigma_1) + \sum_l^{\text{few}} \sqrt{2l+1} P_l(z_2) a_l^{(2)}(\sigma_2) + \sum_l^{\text{few}} \sqrt{2l+1} P_l(z_3) a_l^{(3)}(\sigma_3).$$

Simple **model**:  = $a_l^{(i)}(\sigma_1) \rightarrow c^{(i)} \text{BW}(\sigma_1) = \text{wavy line with orange dot}$.


Partial-waves vs Isobar representation

Isobar representation



$$F(\sigma_1, \sigma_2) = F^{(1)}(\sigma_1, \sigma_2) + F^{(2)}(\sigma_1, \sigma_2) + F^{(3)}(\sigma_1, \sigma_2)$$

$$= \sum_l^{\text{few}} \sqrt{2l+1} P_l(z_1) a_l^{(1)}(\sigma_1) + \sum_l^{\text{few}} \sqrt{2l+1} P_l(z_2) a_l^{(2)}(\sigma_2) + \sum_l^{\text{few}} \sqrt{2l+1} P_l(z_3) a_l^{(3)}(\sigma_3).$$

Simple **model**:  = $a_l^{(i)}(\sigma_1) \rightarrow c^{(i)} \text{BW}(\sigma_1) = \text{wavy line with a small orange circle attached to it.}$

Partial-wave representation

$$\text{wavy line with a small white circle attached to it} = F(\sigma_1, \sigma_2) = \sum_l^{\infty} \sqrt{2l+1} P_l(z_1) f_l^{(1)}(\sigma_1)$$

Why would someone do this? – theoretical constant to $f^{(1)}(\sigma_1)$ is straightforward.

Two-body unitarity and Khuri-Trieman model

Example of $f_0^{(1)}(\sigma_1)$ constraints:

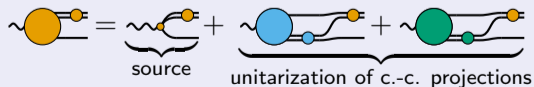
$$f_0^{(1)}(\sigma_1) = \underbrace{a_0^{(1)}(\sigma_1)}_{\text{same channel}} + \underbrace{\int_{-1}^1 \frac{dz_1}{2} \left(\sum_l \sqrt{2l+1} P_l(z_2) a_l^{(2)}(\sigma_2) + \sum_l \sqrt{2l+1} P_l(z_3) a_l^{(3)}(\sigma_3) \right)}_{\text{cross-channel(c.-c.) projections}}$$

Unitarity of $f_0^{(1)}(\sigma_1)$ – same RHC as $2 \rightarrow 2$ scattering amplitude, $BW_0^{(1)}(\sigma_1)$

⇒ consistency relation the **direct term** and the **cross-channel projections**

⇒ $a_l^{(1)}(\sigma_1)$ obtains corrections from one seen in $2 \rightarrow 2$.

KT model: analytic continuation of **two-body** unitarity



(the loop is a dispersive integral)

Diagrammatic representation

Isobar representation with $a_l^{(i)}(\sigma_i) = \hat{a}_l^{(i)}(\sigma_i) BW_l^{(i)}(\sigma_i)$

$$\sim \text{white circle} = \sim \text{orange circle} + \sim \text{blue circle} + \sim \text{green circle}$$

The amplitude prefactor is not constant: $a_l^{(i)}(\sigma_i) = c_l^i BW_l^{(i)}(\sigma_i) + \dots$

$$\begin{aligned} \sim \text{orange circle} &= \sim \text{orange blob} + \\ &+ \sim \text{orange blob with blue blob} + \sim \text{orange blob with green blob} + \\ &+ \sim \text{orange blob with blue and green blobs} + \sim \text{orange blob with blue and white blobs} + \sim \text{orange blob with green and white blobs} + \dots \end{aligned}$$

$$= \sim \text{orange blob} \left[1 + \text{diagram with } \mathcal{L} \right]$$

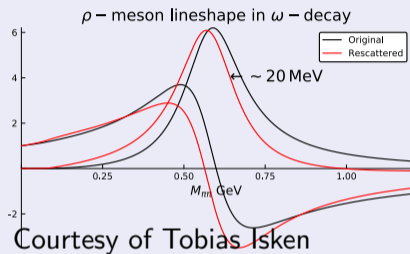
the ladder – a sum of all possible exchanges

$$\sim \text{blue circle} = \sim \text{blue blob} + \sim \text{blue blob with green blob} + \sim \text{blue blob with orange blob} + \dots = \sim \text{blue blob} \left[1 + \text{diagram with } \mathcal{L} \right]$$

$$\sim \text{green circle} = \sim \text{green blob} + \sim \text{green blob with orange blob} + \sim \text{green blob with blue blob} + \dots = \sim \text{green blob} \left[1 + \text{diagram with } \mathcal{L} \right]$$

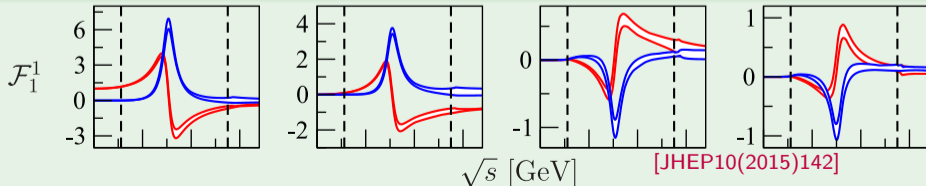
Khuri-Treiman model in practice

Light-meson decays



- $\eta \rightarrow 3\pi$ [Sebastian et al. (2011)], [P.Guo et al., JPAC, 2015], [Albaladejo, Moussallam (2017)]
- $\eta' \rightarrow \eta\pi\pi$ [Isken, Kubis (2017)]
- $\omega/\phi \rightarrow 3\pi$ [Niecknig, Kubis (2012)], [Danilkin et al., JPAC (2012)]
- $a_1 \rightarrow 3\pi$ [JPAC (in progress)]

Open charm, $D \rightarrow K\pi\pi$, [Niecknig, Kubis (2015)], [Moussallam, in progress (2017)]



ρ -meson
lineshape: direct
and induced

Three-particle scattering

Three-body unitarity, Ladders and Resonances, short-range factorization

[[arXiv:1904.11894](https://arxiv.org/abs/1904.11894)]

Decomposition of the $3 \rightarrow 3$ scattering

Decomposition of the $3 \rightarrow 3$ scattering

- **Particle pairing** (symmetrization or isobar decomposition), e.g. for the state of identical particles:

$$\begin{aligned} |p_1 p_2 p_3\rangle &= \frac{1}{3!} (|p_1\rangle \otimes |p_2\rangle \otimes |p_3\rangle + \text{symm.}) \\ &= \frac{1}{3} \sum_{a=1}^3 |p_{a_1}\rangle \frac{|p_{a_2}\rangle \otimes |p_{a_3}\rangle + |p_{a_3}\rangle \otimes |p_{a_2}\rangle}{2} = \frac{1}{3} \sum_{a=1}^3 |a\rangle \quad - \text{isobar-spectator states,} \end{aligned}$$

Decomposition of the $3 \rightarrow 3$ scattering

- **Particle pairing** (symmetrization or isobar decomposition), e.g. for the state of identical particles:

$$\begin{aligned} |p_1 p_2 p_3\rangle &= \frac{1}{3!} (|p_1\rangle \otimes |p_2\rangle \otimes |p_3\rangle + \text{symm.}) \\ &= \frac{1}{3} \sum_{a=1}^3 |p_{a_1}\rangle \frac{|p_{a_2}\rangle \otimes |p_{a_3}\rangle + |p_{a_3}\rangle \otimes |p_{a_2}\rangle}{2} = \frac{1}{3} \sum_{a=1}^3 |a\rangle \quad - \text{isobar-spectator states,} \end{aligned}$$

- Separation of **connected** and **disconnected** terms (LSZ reduction):

$$\text{Diagram} = \sum_9 \left(3 \text{Diagram}_1 + \text{Diagram}_2 \right)$$

Decomposition of the $3 \rightarrow 3$ scattering

- **Particle pairing** (symmetrization or isobar decomposition), e.g. for the state of identical particles:

$$\begin{aligned} |p_1 p_2 p_3\rangle &= \frac{1}{3!} (|p_1\rangle \otimes |p_2\rangle \otimes |p_3\rangle + \text{symm.}) \\ &= \frac{1}{3} \sum_{a=1}^3 |p_{a_1}\rangle \frac{|p_{a_2}\rangle \otimes |p_{a_3}\rangle + |p_{a_3}\rangle \otimes |p_{a_2}\rangle}{2} = \frac{1}{3} \sum_{a=1}^3 |a\rangle \quad - \text{isobar-spectator states,} \end{aligned}$$

- Separation of **connected** and **disconnected** terms (LSZ reduction):

$$\text{Diagram} = \sum_9 \left(3 \text{Diagram} + \text{Diagram} \right)$$

- Partial wave **expansion** (spin l in subchannels, spin j overall)

Decomposition of the $3 \rightarrow 3$ scattering

- **Particle pairing** (symmetrization or isobar decomposition), e.g. for the state of identical particles:

$$\begin{aligned}
 |p_1 p_2 p_3\rangle &= \frac{1}{3!} (|p_1\rangle \otimes |p_2\rangle \otimes |p_3\rangle + \text{symm.}) \\
 &= \frac{1}{3} \sum_{a=1}^3 |p_{a_1}\rangle \frac{|p_{a_2}\rangle \otimes |p_{a_3}\rangle + |p_{a_3}\rangle \otimes |p_{a_2}\rangle}{2} = \frac{1}{3} \sum_{a=1}^3 |a\rangle \quad - \text{isobar-spectator states,}
 \end{aligned}$$

- Separation of **connected** and **disconnected** terms (LSZ reduction):

$$\text{Diagram} = \sum_9 \left(3 \text{Diagram} + \text{Diagram} \right)$$

- Partial wave **expansion** (spin l in subchannels, spin j overall)
- **Amputation** of the last scattering bit

$$\begin{aligned}
 \text{Diagram} &= t(\sigma), \\
 \text{Diagram} &\equiv \text{Diagram} = t(\sigma') \mathcal{T}(\sigma', s, \sigma) t(\sigma),
 \end{aligned}$$

Three-body-unitarity constraint

[G.Fleming, Phys.Rev. 135 (1964)]

Three-body scattering amplitude must satisfy the integral equation

$$\mathcal{T}(\sigma', s, \sigma) - \mathcal{T}^\dagger(\sigma', s, \sigma) =$$

$$2i \frac{1}{\lambda_s^{1/2}(\sigma')} \frac{1}{8\pi} \int_{\sigma^-(\sigma', s)}^{\sigma^+(\sigma', s)} d\sigma'_3 t(\sigma'_3) \mathcal{T}(\sigma'_3, s, \sigma)$$

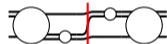
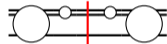
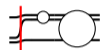
$$+ \frac{i}{3} \int_{4m_\pi^2}^{(\sqrt{s}-m_\pi)^2} \frac{d\sigma''}{2\pi} \mathcal{T}^\dagger(\sigma', s, \sigma'') t(\sigma'') t^\dagger(\sigma'') \rho(\sigma'') \rho_s(\sigma'') \mathcal{T}(\sigma'', s, \sigma)$$

$$+ \frac{2i}{3} \frac{1}{(8\pi)^2} \iint_{\phi(\sigma''_2, s, \sigma''_3) > 0} \frac{d\sigma''_2 d\sigma''_3}{2\pi s} \mathcal{T}^\dagger(\sigma', s, \sigma''_2) t^\dagger(\sigma''_2) t(\sigma''_3) \mathcal{T}(\sigma''_3, s, \sigma)$$

$$+ 2i \frac{1}{\lambda_s^{1/2}(\sigma)} \frac{1}{8\pi} \int_{\sigma^-(\sigma, s)}^{\sigma^+(\sigma, s)} d\sigma_2 \mathcal{T}^\dagger(\sigma', s, \sigma_2) t^\dagger(\sigma_2)$$

$$+ 6i \frac{2\pi s}{\lambda_s^{1/2}(\sigma') \lambda_s^{1/2}(\sigma)} \theta^+(\phi(\sigma', s, \sigma)).$$

$$\text{Diagram 1} - \text{Diagram 2}^\dagger =$$



In a short form: [Aaron-Amada(TCP 2 (1977)), Mai et al.(EPJ A53 (2017)), Jackura et al.(EPJ C79 (2019))]:

$$\mathcal{T} - \mathcal{T}^\dagger = \mathcal{D}_\tau \mathcal{T} + \mathcal{T}^\dagger (\tau - \tau^\dagger) \mathcal{T} + \mathcal{T}^\dagger \tau^\dagger \mathcal{D}_\tau \mathcal{T} + \mathcal{T}^\dagger \tau^\dagger \mathcal{D} + \mathcal{D},$$

Splitting amplitude by the interaction range

$$\text{Diagram} \quad \mathcal{T}(\sigma', s, \sigma) = \mathcal{L}(\sigma', s, \sigma) + \mathcal{R}(\sigma', s, \sigma). \quad \text{Diagram} + \text{Diagram}$$

Long-range part: exchange processes (on-shell) [Mai et al.(EPJ A53 (2017))]

- Infinite sum of the one-particle-exchange process

$$\text{Diagram} \quad \mathcal{L} = \mathcal{B} + \mathcal{L}\tau\mathcal{B} = \mathcal{B} + \mathcal{B}\tau\mathcal{L} \quad \text{Diagram} + \text{Diagram}$$

- $\mathcal{T} = \mathcal{L}$, $\mathcal{R} = 0$ already satisfy unitarity. Can it have resonances?

Short-range part: resonances [MM, Y.Wunderlich, et al. (JPAC) 1904.11894]

- Condition for $\mathcal{R}(\sigma', s, \sigma)$ is complicated
- However, simplified significantly if FSI is factorized from both sides:

$$\text{Diagram} \quad \mathcal{R} \equiv (1 + \mathcal{L}\tau)\hat{\mathcal{R}}(\tau\mathcal{L} + 1). \quad \left(\text{Diagram} + \text{Diagram} \right) \text{Diagram} \left(\text{Diagram} + \text{Diagram} \right),$$

Unitarity constraint for the resonance kernel

Familiar form of the constraint (see two-body constraint at slide 4):

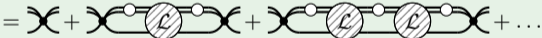
$$\begin{aligned}\widehat{\mathcal{R}} - \widehat{\mathcal{R}}^\dagger &= \widehat{\mathcal{R}}^\dagger (1 + \tau^\dagger \mathcal{L}^\dagger) \left[\tau - \tau^\dagger + \tau^\dagger \mathcal{D} \tau \right] (1 + \mathcal{L} \tau) \widehat{\mathcal{R}} \\ &= \widehat{\mathcal{R}}^\dagger \left[\tau - \tau^\dagger + \tau \mathcal{L} \tau - \tau^\dagger \mathcal{L}^\dagger \tau^\dagger \right] \widehat{\mathcal{R}}.\end{aligned}$$

Unitarity constraint for the resonance kernel

Familiar form of the constraint (see two-body constraint at slide 4):

$$\begin{aligned}\widehat{\mathcal{R}} - \widehat{\mathcal{R}}^\dagger &= \widehat{\mathcal{R}}^\dagger (1 + \tau^\dagger \mathcal{L}^\dagger) \left[\tau - \tau^\dagger + \tau^\dagger \mathcal{D} \tau \right] (1 + \mathcal{L} \tau) \widehat{\mathcal{R}} \\ &= \widehat{\mathcal{R}}^\dagger \left[\tau - \tau^\dagger + \tau \mathcal{L} \tau - \tau^\dagger \mathcal{L}^\dagger \tau^\dagger \right] \widehat{\mathcal{R}}.\end{aligned}$$

- K-matrix-like solution (cf. $K_{d.f.}$ [M.Hansen, S.Sharpe, PRD90 (2014), 116003])

$$\begin{aligned}\widehat{\mathcal{R}} &= \mathcal{X} + \mathcal{X}(\tau + \tau \mathcal{L} \tau) \widehat{\mathcal{R}} \\ &= \mathcal{X} + \mathcal{X}(\tau + \tau \mathcal{L} \tau) \mathcal{X} + \mathcal{X}(\tau + \tau \mathcal{L} \tau) \mathcal{X}(\tau + \tau \mathcal{L} \tau) \mathcal{X} + \dots \\ &= \text{diagrammatic expansion} + \dots\end{aligned}$$


Unitarity constraint for the resonance kernel

Familiar form of the constraint (see two-body constraint at slide 4):

$$\begin{aligned}\widehat{\mathcal{R}} - \widehat{\mathcal{R}}^\dagger &= \widehat{\mathcal{R}}^\dagger (1 + \tau^\dagger \mathcal{L}^\dagger) \left[\tau - \tau^\dagger + \tau^\dagger \mathcal{D} \tau \right] (1 + \mathcal{L} \tau) \widehat{\mathcal{R}} \\ &= \widehat{\mathcal{R}}^\dagger \left[\tau - \tau^\dagger + \tau \mathcal{L} \tau - \tau^\dagger \mathcal{L}^\dagger \tau^\dagger \right] \widehat{\mathcal{R}}.\end{aligned}$$

- K-matrix-like solution (cf. $K_{d.f.}$ [M.Hansen, S.Sharpe, PRD90 (2014), 116003])

$$\begin{aligned}\widehat{\mathcal{R}} &= \mathcal{X} + \mathcal{X}(\tau + \tau \mathcal{L} \tau) \widehat{\mathcal{R}} \\ &= \mathcal{X} + \mathcal{X}(\tau + \tau \mathcal{L} \tau) \mathcal{X} + \mathcal{X}(\tau + \tau \mathcal{L} \tau) \mathcal{X}(\tau + \tau \mathcal{L} \tau) \mathcal{X} + \dots \\ &= \text{diagrammatic expansion}\end{aligned}$$

- Rescattering interpretation [MM, Y.Wunderlich, et al. (JPAC) 1904.11894]:

$$\widehat{\mathcal{R}} - \widehat{\mathcal{R}}^\dagger = \underbrace{\widehat{\mathcal{R}}^\dagger (1 + \tau^\dagger \mathcal{L}^\dagger)}_{\text{rescattering}} \overbrace{\left[\tau - \tau^\dagger + \tau^\dagger \mathcal{D} \tau \right]}^{\text{direct+crossed coupling}} \underbrace{(1 + \mathcal{L} \tau) \widehat{\mathcal{R}}}_{\text{rescattering}} \xrightarrow{\text{sort-of}} \text{diagrammatic expansion}$$

Factorization of the resonance kernel

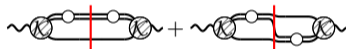
- Strictly, one more (weak) assumption – **Factorization**

$$\begin{aligned}\widehat{\mathcal{R}}(\sigma', s, \sigma) &= k_f(\sigma') \widehat{\mathcal{R}}(s) k_i(\sigma) \quad \text{OR} \\ &= \widehat{\mathcal{R}}_{00}(s) + \sigma' \widehat{\mathcal{R}}_{10}(s) + \widehat{\mathcal{R}}_{01}(s) \sigma + \sigma' \widehat{\mathcal{R}}_{11}(s) \sigma + \dots,\end{aligned}$$

⇒ Unitarity requirement is algebraic!

$$\widehat{\mathcal{R}}(s) - \widehat{\mathcal{R}}^\dagger(s) = i \widehat{\mathcal{R}}^\dagger(s) \Sigma(s) \widehat{\mathcal{R}}(s),$$

with $\Sigma \equiv \mathcal{K}^\dagger(\tau - \tau^\dagger)\mathcal{K} + \mathcal{K}^\dagger \tau^\dagger \mathcal{D} \tau \mathcal{K},$



\mathcal{K} is the modification of the isobar lineshape due to the rescattering

Factorization of the resonance kernel

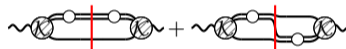
- Strictly, one more (weak) assumption – **Factorization**

$$\begin{aligned}\widehat{\mathcal{R}}(\sigma', s, \sigma) &= k_f(\sigma') \widehat{\mathcal{R}}(s) k_i(\sigma) \text{ OR} \\ &= \widehat{\mathcal{R}}_{00}(s) + \sigma' \widehat{\mathcal{R}}_{10}(s) + \widehat{\mathcal{R}}_{01}(s) \sigma + \sigma' \widehat{\mathcal{R}}_{11}(s) \sigma + \dots,\end{aligned}$$

⇒ Unitarity requirement is algebraic!

$$\widehat{\mathcal{R}}(s) - \widehat{\mathcal{R}}^\dagger(s) = i \widehat{\mathcal{R}}^\dagger(s) \Sigma(s) \widehat{\mathcal{R}}(s),$$

with $\Sigma \equiv \mathcal{K}^\dagger(\tau - \tau^\dagger)\mathcal{K} + \mathcal{K}^\dagger \tau^\dagger \mathcal{D} \tau \mathcal{K},$



\mathcal{K} is the modification of the isobar lineshape due to the rescattering

An approximate-three-body unitarity

$$\widehat{\mathcal{R}}(s) = \frac{g^2}{m^2 - s - ig^2/2 \left[\text{diagram} + \text{diagram} \right]}$$

contains effect of the subchannel-resonances **interference**

The quasi-two-body approximation

[J.Basdevant, Ed Berger, PRD19 (1979) 239]

$$\widehat{\mathcal{R}}(s) = \frac{g^2}{m^2 - s - ig^2/2 \left[\text{diagram} \right]}$$

naively accounts for the subchannel-resonance decay

Analysis of $a_1(1260)$

subchannel-resonance interference, analytic continuation

[PRD98 (2018), 096021]

$a_1(1260)$ state – ground axial vector – isospin partner of ρ [PDG (2018)]

$a_1(1260)$ WIDTH

INSPIRE search

VALUE (MeV)	EVTS	DOCUMENT ID	TECN	COMMENT
250 to 600	OUR ESTIMATE			
389 ± 29	OUR AVERAGE	Error includes scale factor of 1.3.		
430 ± 24 ± 31		DARGENT 2017	RVUE	$D^0 \rightarrow \pi^- \pi^+ \pi^- \pi^+$
367 ± 9 ⁺²⁸ ₋₂₅	420k	ALEKSEEV 2010	COMP	190 $\pi^- \rightarrow \pi^- \pi^- \pi^+ P b'$
••• We do not use the following data for averages, fits, limits, etc. •••				
410 ± 31 ± 30		1 AUBERT 2007AU	BABR	10.6 $e^+ e^- \rightarrow \rho^0 \rho^+ \pi^- \gamma$
520 - 680	6360	2 LINK 2007A	FOCS	$D^0 \rightarrow \pi^- \pi^+ \pi^- \pi^+$
480 ± 20		3 GOMEZ-DUMM 2004	RVUE	$\tau^+ \rightarrow \pi^+ \pi^+ \pi^- \nu_\tau$
580 ± 41	90k	SALVINI 2004	OBLX	$\bar{p} p \rightarrow 2 \pi^+ 2 \pi^-$
460 ± 85	205	4 DRUTSKOY 2002	BELL	$B^{(*)} K^- K^0$
814 ± 36 ± 13	37k	5 ASNER 2000	CLE2	10.6 $e^+ e^- \rightarrow \tau^+ \tau^-$, $\tau^- \rightarrow \pi^- \pi^0 \pi^0 \nu_\tau$

$a_1(1260)$ state – ground axial vector – isospin partner of ρ [PDG (2018)]

$a_1(1260)$ WIDTH

INSPIRE search

VALUE (MeV)	EVTS	DOCUMENT ID	TECN	COMMENT
250 to 600	OUR ESTIMATE			
380 ± 20	OUR AVERAGE	Error includes scale factor of 1.3.		
430 ±24 ±31		DARGENT 2017	RVUE	$D^0 \rightarrow \pi^- \pi^+ \pi^- \pi^+$
367 ±9 ⁺²⁸ ₋₂₅	420k	ALEKSEEV 2010	COMP	190 $\pi^- \rightarrow \pi^- \pi^- \pi^+ P b'$
••• We do not use the following data for averages, fits, limits, etc. •••				
410 ±31 ±30		1 AUBERT 2007AU	BABR	10.6 $e^+ e^- \rightarrow \rho^0 \rho^+ \pi^+ \gamma$
520 - 680	6360	2 LINK 2007A	FOCS	$D^0 \rightarrow \pi^- \pi^+ \pi^- \pi^+$
480 ±20		3 GOMEZ-DUMM 2004	RVUE	$\tau^+ \rightarrow \pi^+ \pi^+ \pi^- \nu_\tau$
580 ±41	90k	SALVINI 2004	OBLX	$\bar{p} p \rightarrow 2 \pi^+ 2 \pi^-$
460 ±85	205	4 DRUTSKOY 2002	BELL	$B^{(*)} K^- K^0$
814 ±36 ±13	37k	5 ASNER 2000	CLE2	10.6 $e^+ e^- \rightarrow \tau^+ \tau^-$, $\tau^- \rightarrow \pi^- \pi^0 \pi^0 \nu_\tau$

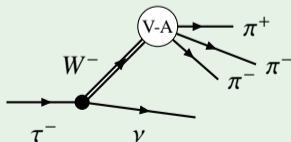
$a_1(1260)$ state – ground axial vector – isospin partner of ρ [PDG (2018)]

$a_1(1260)$ WIDTH

INSPIRE search

VALUE (MeV)	EVTS	DOCUMENT ID	TECN	COMMENT
250 to 600	OUR ESTIMATE			
380 ± 20	OUR AVERAGE Error includes scale factor of 1.3.			
430 ± 24 ± 31		DARGENT 2017	RVUE	$D^0 \rightarrow \pi^- \pi^+ \pi^- \pi^+$
367 ± 9 ⁺²⁸ ₋₂₅	420k	ALEKSEEV 2010	COMP	$190 \pi^- \rightarrow \pi^- \pi^- \pi^+ Pb'$
••• We do not use the following data for averages, fits, limits, etc. •••				
410 ± 31 ± 30		1 AUBERT 2007AU	BABR	$10.6 e^+ e^- \rightarrow \rho^0 \rho^+ \pi^+ \gamma$
520 - 680	6360	2 LINK 2007A	FOCS	$D^0 \rightarrow \pi^- \pi^+ \pi^- \pi^+$
480 ± 20		3 GOMEZ-DUMM 2004	RVUE	$\tau^+ \rightarrow \pi^+ \pi^+ \pi^- \nu_\tau$
580 ± 41	90k	SALVINI 2004	OBLX	$\bar{p} p \rightarrow 2 \pi^+ 2 \pi^-$
460 ± 85	205	4 DRUTSKOY 2002	BELL	$B^{(*)} K^- K^0$
814 ± 36 ± 13	37k	5 ASNER 2000	CLE2	$10.6 e^+ e^- \rightarrow \tau^+ \tau^-, \tau^- \rightarrow \pi^- \pi^0 \pi^0 \nu_\tau$

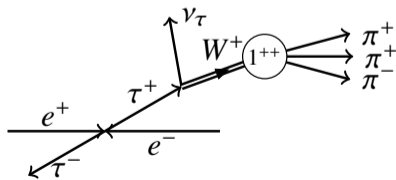
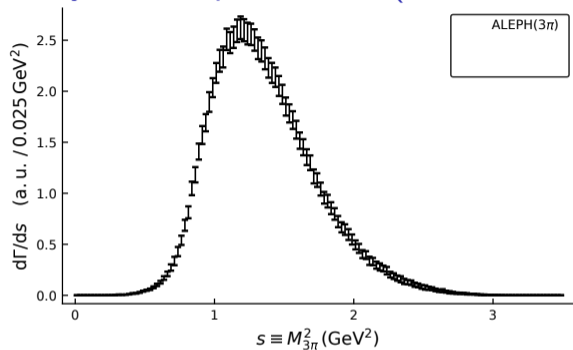
Clean
 $J^{PC} = 1^{++}$



- V-A: Vector (1^{--}) or Axial (1^{++})
- Isospin 1 due to the charge
- Negative G-parity \Rightarrow positive C-parity

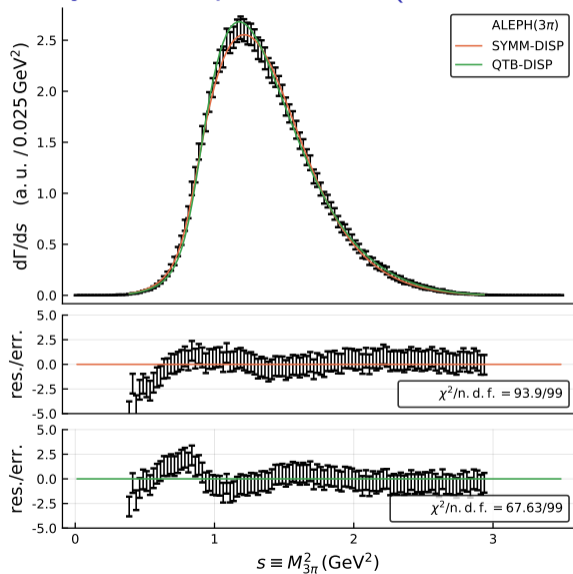
Analysis of experimental (ALEPH measurements)

[data from Phys.Rept.421 (2005)]



Analysis of experimental (ALEPH 3π measurements)

[data from Phys.Rept.421 (2005)]



Two models of $\rho\pi$ scattering:

- SYMM-DISP: Approximate three-body unitarity (includes interference)

$$\Sigma(s) = \left[\text{diagram 1} + \text{diagram 2} \right]$$

The diagram shows two Feynman diagrams for $\rho\pi$ scattering. Each diagram consists of a wavy line (representing a ρ meson) and a solid line (representing a π meson) forming a loop. A vertical red line is drawn through the loop, representing a cut in the complex plane. The two diagrams are summed together.

- QTB-DISP: Quasi-two-body unitarity

$$\Sigma(s) = \left[\text{diagram} \right]$$

The diagram shows a single Feynman diagram for $\rho\pi$ scattering, similar to the one above, but with only one term in the sum.

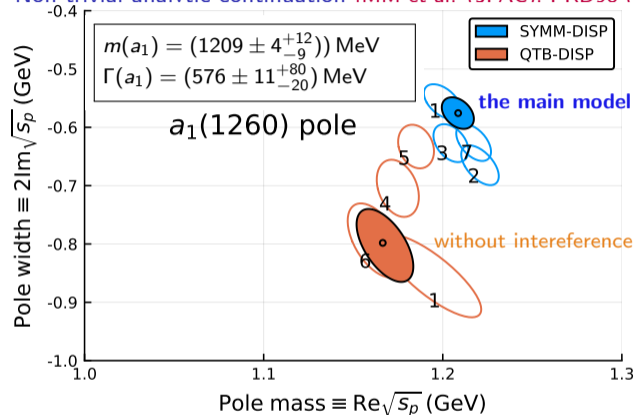
both neglect rescattering, $\mathcal{K} \rightarrow 1$.

Fit to the public data

- Stat. cov. matrix is used in the fit
- Syst. cov. matrix – in the bootstrap

Determination of the $a_1(1260)$ pole position

Non-trivial analytic continuation [IMM et al. (JPAC). PRD98 (2018), 096021]



#	Fit studies
1	$s < 2 \text{ GeV}^2$
2	$R' = 3 \text{ GeV}^{-1}$
3	$m'_\rho = m_\rho + 10 \text{ MeV}$
4	$m'_\rho = m_\rho - 10 \text{ MeV}$
5	$m'_\rho = m_\rho - 20 \text{ MeV}$
6	$\Gamma'_\rho = \Gamma_\rho + 5 \text{ MeV}$
7	$\Gamma'_\rho = \Gamma_\rho - 30 \text{ MeV}$

- Large systematic uncertainties due to disregard of rescattering effects
- Effect of the subchannel-resonances interference is very important

Summary

- **Unitarity** is an important constraint
 - ▶ that guides the amplitude construction
[Mai et al.(EPJ A53 (2017)), Jackura et al.(EPJ C79 (2019)), MM et al. (JPAC) 1904.11894]
 - ▶ is satisfied in a good FT consideration [R.Briceno, 1905.11188]
 - ▶ Separation between the short-range and the long-range is not unique [M.Doering et al., PLB681 (2009) 26-31]
 - ▶ Decomposition of the short-range is not unique [A.Jackura et al., 1905.12007]
- The **ladder** is a new phenomenon of the three-particle physics
 - ▶ sum of particle exchange diagrams
 - ▶ left-hand singularity in the physical region
 - ▶ genuine non-factorizable component
- The **resonance** part admits Factorization:
 - ▶ Effect of the **Ladder** is the common final-state interaction
 - ▶ Unitarity requirement casts to the familiar two-body-like form.

Summary

- **Unitarity** is an important constraint
 - ▶ that guides the amplitude construction [Mai et al.(EPJ A53 (2017)), Jackura et al.(EPJ C79 (2019)), MM et al. (JPAC) 1904.11894]
 - ▶ is satisfied in a good FT consideration [R.Briceno, 1905.11188]
 - ▶ Separation between the short-range and the long-range is not unique [M.Doering et al., PLB681 (2009) 26-31]
 - ▶ Decomposition of the short-range is not unique [A.Jackura et al., 1905.12007]

- The **ladder** is a new phenomenon of the three-particle physics

Outlook

Better understanding of the exchange processes is needed:

- ⇒ studies of the final-state interaction in the decays
- ⇒ studies of the fix-target production data (COMPASS, GlueX)
- ⇒ **studies of the nice, clean scattering data from the lattice**

Thank you for attention

Thanks to my collaborators (JPAC group):



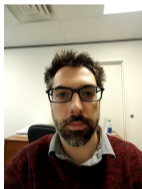
Yannick
Wundelich



Andrew
Jakura



Alessandro
Pilloni



Vincent
Mathieu



Miguel
Albaladejo



Cesar
Fernandez



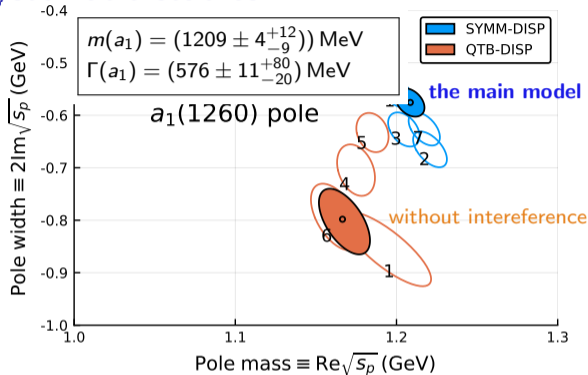
Bernhard
Ketzer



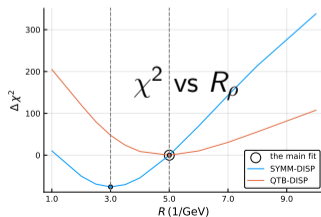
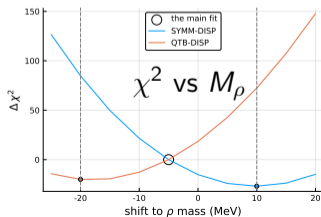
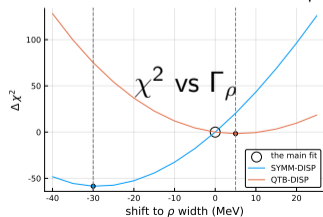
Adam
Szczepaniak

Backup

Systematic studies



#	Fit studies
1	$s < 2 \text{ GeV}^2$
2	$R' = 3 \text{ GeV}^{-1}$
3	$m'_\rho = m_\rho + 10 \text{ MeV}$
4	$m'_\rho = m_\rho - 10 \text{ MeV}$
5	$m'_\rho = m_\rho - 20 \text{ MeV}$
6	$\Gamma'_\rho = \Gamma_\rho + 5 \text{ MeV}$
7	$\Gamma'_\rho = \Gamma_\rho - 30 \text{ MeV}$



Tour to the complex plane

[MM (JPAC), PRD98 (2018), 096021]

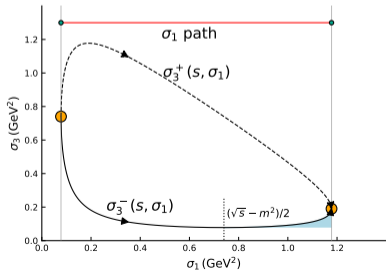
Analytical continuation

$$|t_{\parallel}^{-1}(s)| = \left| \frac{m^2 - s}{g^2} - i \left(\frac{\tilde{\rho}(s)}{2} + \rho(s) \right) \right|.$$

- Analytical continuation of $\rho(s)$: integral over the Dalitz plot for the complex energy

$$\rho(s) = \sum_{\lambda} \int d\Phi_3 \left| f_{\rho}(\sigma_1) d_{\lambda 0}(\theta_{23}) - f_{\rho}(\sigma_3) d_{\lambda 0}(\hat{\theta}_3 + \theta_{12}) \right|^2$$

- Analytic continuation of ρ -meson decay amplitude f_{ρ}



Tour to the complex plane

[MM (JPAC), PRD98 (2018), 096021]

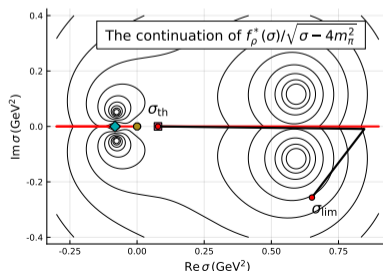
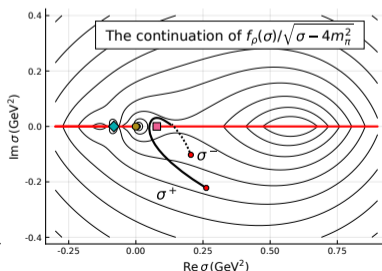
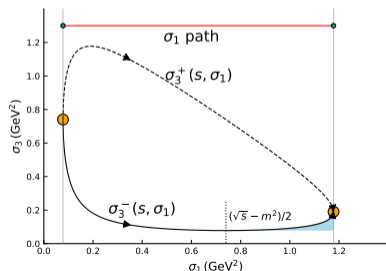
Analytical continuation

$$|t_{\parallel}^{-1}(s)| = \left| \frac{m^2 - s}{g^2} - i \left(\frac{\tilde{\rho}(s)}{2} + \rho(s) \right) \right|.$$

- Analytical continuation of $\rho(s)$: integral over the Dalitz plot for the complex energy

$$\rho(s) = \sum_{\lambda} \int d\Phi_3 \left| f_{\rho}(\sigma_1) d_{\lambda 0}(\theta_{23}) - f_{\rho}(\sigma_3) d_{\lambda 0}(\hat{\theta}_3 + \theta_{12}) \right|^2$$

- Analytic continuation of ρ -meson decay amplitude f_{ρ}



Tour to the complex plane

[MM (JPAC), PRD98 (2018), 096021]

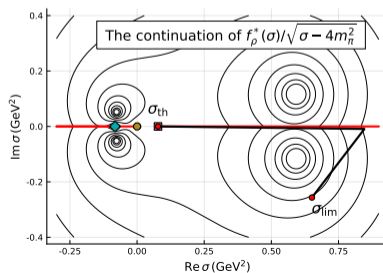
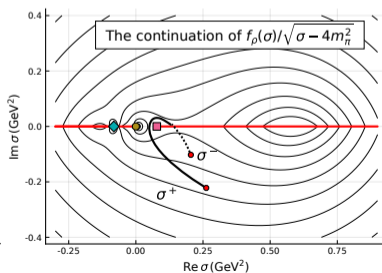
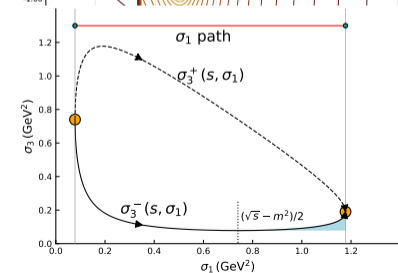
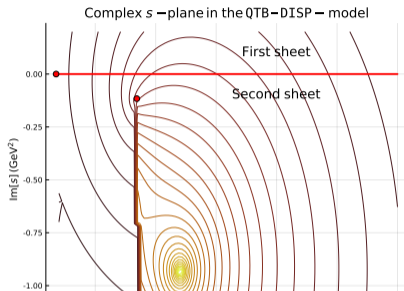
Analytical continuation

$$|t_{\parallel}^{-1}(s)| = \left| \frac{m^2 - s}{g^2} - i \left(\frac{\tilde{\rho}(s)}{2} + \rho(s) \right) \right|.$$

- Analytical continuation of $\rho(s)$: integral over the Dalitz plot for the complex energy

$$\rho(s) = \sum_{\lambda} \int d\Phi_3 \left| f_{\rho}(\sigma_1) d_{\lambda 0}(\theta_{23}) - f_{\rho}(\sigma_3) d_{\lambda 0}(\hat{\theta}_3 + \theta_{12}) \right|^2$$

- Analytical continuation of ρ -meson decay amplitude f_{ρ}



Tour to the complex plane

[MM (JPAC), PRD98 (2018), 096021]

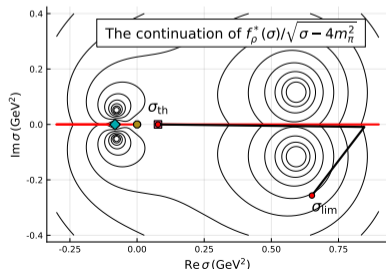
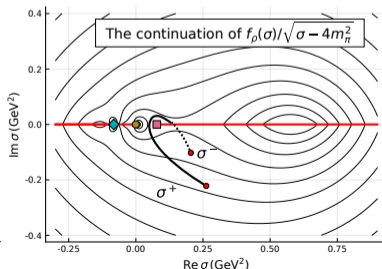
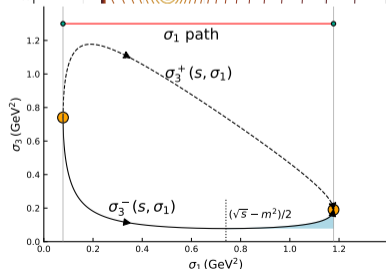
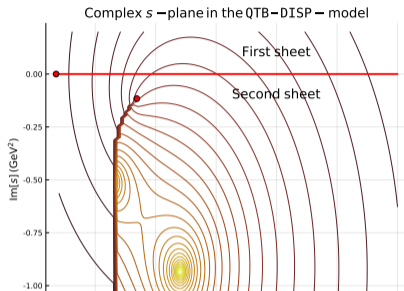
Analytical continuation

$$|t_{\parallel}^{-1}(s)| = \left| \frac{m^2 - s}{g^2} - i \left(\frac{\tilde{\rho}(s)}{2} + \rho(s) \right) \right|.$$

- Analytical continuation of $\rho(s)$: integral over the Dalitz plot for the complex energy

$$\rho(s) = \sum_{\lambda} \int d\Phi_3 \left| f_{\rho}(\sigma_1) d_{\lambda 0}(\theta_{23}) - f_{\rho}(\sigma_3) d_{\lambda 0}(\hat{\theta}_3 + \theta_{12}) \right|^2$$

- Analytic continuation of ρ -meson decay amplitude f_{ρ}



Tour to the complex plane

[MM (JPAC), PRD98 (2018), 096021]

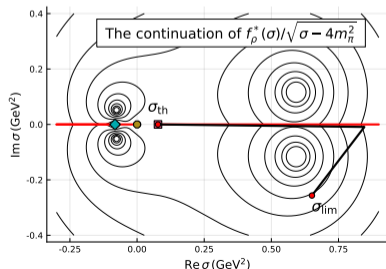
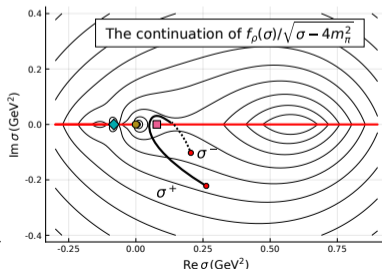
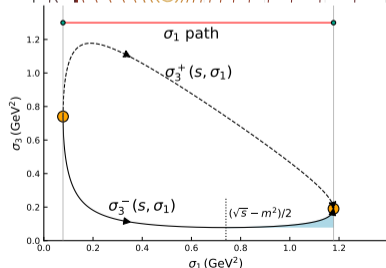
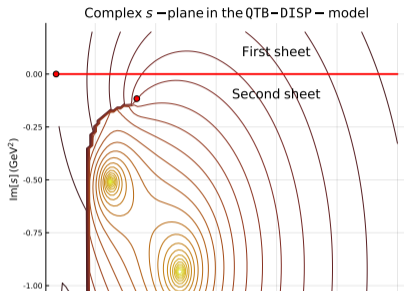
Analytical continuation

$$|t_{\parallel}^{-1}(s)| = \left| \frac{m^2 - s}{g^2} - i \left(\frac{\tilde{\rho}(s)}{2} + \rho(s) \right) \right|.$$

- Analytical continuation of $\rho(s)$: integral over the Dalitz plot for the complex energy

$$\rho(s) = \sum_{\lambda} \int d\Phi_3 \left| f_{\rho}(\sigma_1) d_{\lambda 0}(\theta_{23}) - f_{\rho}(\sigma_3) d_{\lambda 0}(\hat{\theta}_3 + \theta_{12}) \right|^2$$

- Analytic continuation of ρ -meson decay amplitude f_{ρ}



Tour to the complex plane

[MM (JPAC), PRD98 (2018), 096021]

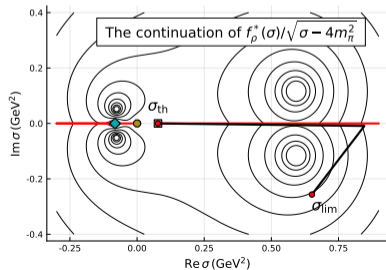
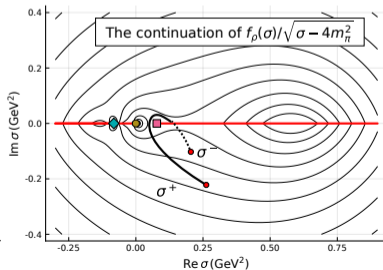
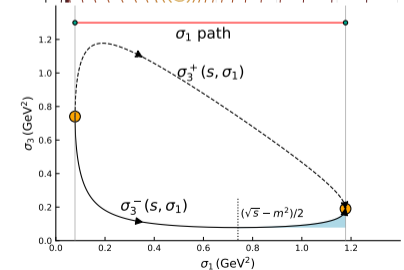
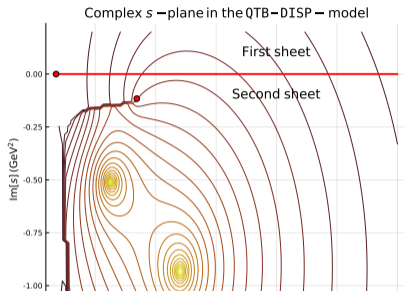
Analytical continuation

$$|t_{\parallel}^{-1}(s)| = \left| \frac{m^2 - s}{g^2} - i \left(\frac{\tilde{\rho}(s)}{2} + \rho(s) \right) \right|.$$

- Analytical continuation of $\rho(s)$: integral over the Dalitz plot for the complex energy

$$\rho(s) = \sum_{\lambda} \int d\Phi_3 \left| f_{\rho}(\sigma_1) d_{\lambda 0}(\theta_{23}) - f_{\rho}(\sigma_3) d_{\lambda 0}(\hat{\theta}_3 + \theta_{12}) \right|^2$$

- Analytic continuation of ρ -meson decay amplitude f_{ρ}



The spurious pole in the Breit-Wigner model

Energy dependent width, stable particles

$$t(s) = \frac{1}{m^2 - s - im\Gamma(s)}, \quad \Gamma(s) = \Gamma_0 \frac{p(s)}{p(m^2)} \frac{m}{\sqrt{s}}, \quad p(s) = \frac{\sqrt{(s - (m_1 + m_2)^2)(s - (m_1 - m_2)^2)}}{2\sqrt{s}}.$$

Example: $m_1 = 140$ MeV, $m_2 = 770$ MeV, $m = 1.26$ GeV, $\Gamma_0 = 0.5$ GeV

